



Cite this: RSC Adv., 2018, 8, 37643

Design, synthesis, and bioactivity evaluation of antitumor sorafenib analogues

Shiyang Zhou  ^{ab} and Guangying Chen ^{*ab}

Malignant tumors are a serious threat to human health and are generally treated with chemical therapy. This chemical therapy uses agents that act on signal transduction pathway mechanism of tumor with good selectivity and low toxicity. Sorafenib is a multikinase target inhibitor with good tumor inhibitory activity and a protein kinase inhibitor. In this research, a novel series of sorafenib analogues and derivatives were designed, synthesized, and evaluated as tumor inhibitors. These compounds used sorafenib as the lead compound and achieved modifications using bioisosteres and the alkyl principle. The *in vitro* results showed that compounds **3c**, **3d**, **3h**, **3n**, **3r**, and **3z** had good inhibitory effects on human cervical cancer cells (HeLa), while compounds **3t** and **3v** had good inhibitory effects on human lung cancer cells (H1975 and A549). Among these, compound **3d** had an inhibitory activity (IC_{50}) of $0.56 \pm 0.04 \mu\text{mol L}^{-1}$ against HeLa cells (human cervical cancer), the compound **3t** had an IC_{50} of $2.34 \pm 0.07 \mu\text{mol L}^{-1}$ against H1975 cells (human lung cancer), and compound **3v** had an IC_{50} of $1.35 \pm 0.03 \mu\text{mol L}^{-1}$ against A549 cells (human lung cancer). The *in vivo* results showed that these compounds had good antitumor effects and low acute toxicity.

Received 5th October 2018
Accepted 23rd October 2018

DOI: 10.1039/c8ra08246d

rsc.li/rsc-advances

1. Introduction

A malignant tumor is a common disease that seriously threatens human health. The number of deaths caused by malignant tumors is second only to cerebrovascular disease among all diseases.^{1–3} General treatment methods for tumors include surgical, radiation, chemical (drug therapy), and biological treatments. However, chemotherapy and surgical treatment remain the most common treatment methods.^{4–7} Antitumor drugs have advanced considerably since the discovery of mechlorethamine in the 1940s, which was used to treat malignant tumors.^{8–13} In the last twenty years, the development of molecular biology and cell biology have further improved understanding of tumor biological mechanisms, and research into antitumor drugs has provided new targets.^{14–18} The batch production of new chemical structures or drugs with unique mechanisms of action for clinical tumor treatment has provided highly efficient and low-toxicity drugs.^{19–21}

Antitumor drugs currently used in clinical practice can be divided into four categories according to their mechanism of action: (i) agents that directly act on DNA; (ii) agents that interfere with DNA synthesis; (iii) antimitotic agents; and (iv) agents that affect the signal transduction pathway mechanism of tumors.^{22–24} Among these antitumor drugs, types (i)–(iii) all

influence DNA synthesis or cell mitosis.²⁵ Therefore, these antitumor drugs have strong effects, but lack selectivity and have significant toxic effects. More selective, efficient, and less toxic antitumor drugs that interfere with or directly act on specific biological processes in tumor cells have long been sought.^{26–28} With the development of life science, biological mechanisms related to the occurrence and development of tumors have gradually been elucidated.²⁹ As a result, research into antitumor drugs has begun to move towards targeted rational drug design, with some new high-selectivity drugs produced.³⁰

The reversible phosphorylation of protein amino acid side chains is an important mechanism for the regulation of enzyme and signal protein activity.³¹ Protein kinase and protein phosphatase are involved in reversible phosphorylation and play key roles in regulating metabolism, gene expression, cell growth, cell division, and cell differentiation. Protein kinase is a phosphotransferase that catalyzes the transfer of phosphate groups from ATP to protein receptor amino acids.^{32,33} Tyrosine kinase is the most important protein kinase, while protein tyrosine kinase is a type of protein that shows tyrosine kinase activity, including receptor-type and nonreceptor-type proteins.³⁴ Receptor-type proteins include epidermal growth factor receptor (EGFR), vascular endothelial growth factor receptor (VEGFR), platelet-derived growth factor receptor (PDGFR), insulin receptor (InsR), and fibroblast growth factor receptor (FGFR). Nonreceptor-type proteins include Src, Abl, Jak, Csk, Fak, and Fes. Protein tyrosine kinase dysfunction can cause many diseases.^{35–37} Some data have shown that over 50% of

^aCollege of Chemistry and Chemical Engineering, Hainan Normal University, Haikou 571158, China. E-mail: chgying123@163.com

^bKey Laboratory of Tropical Medicinal Plant Chemistry of Ministry of Education, Hainan Normal University, Haikou 571158, China



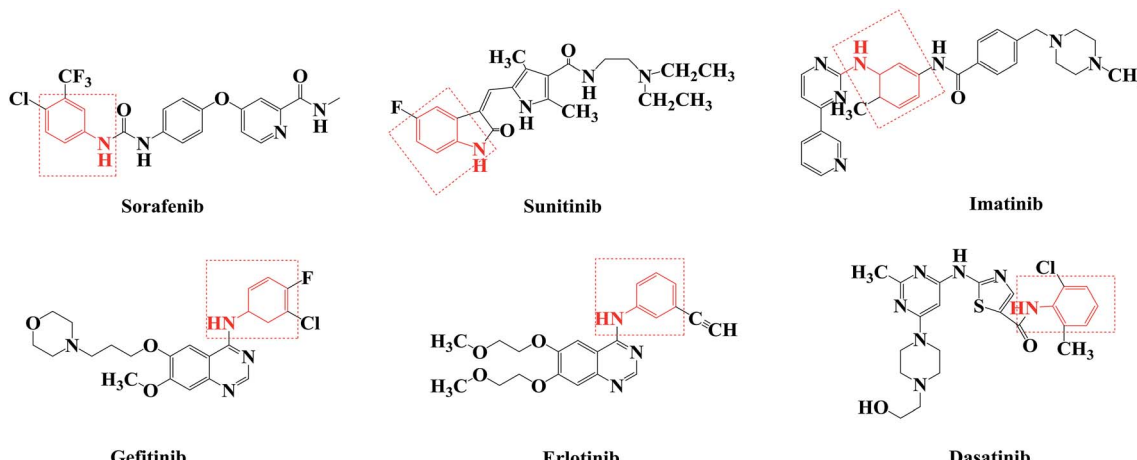


Fig. 1 Structures of protein kinase inhibitors.

protooncogenes and oncogene products have protein tyrosine kinase activity, and that their abnormal expression leads to cell proliferation and regulation disorders, which cause tumors. Furthermore, abnormal expression of tyrosine kinase is closely related to tumor invasion and metastasis, tumor angiogenesis, and tumor chemotherapy resistance.^{38–41} In recent years, protein tyrosine kinase has become the target of drug action. The design of protein kinase inhibitors that can interfere with the cell signal transduction pathway has been used in the search for disease drug treatments.^{42–45}

Agents that act on the signal transduction pathway mechanism in tumors include protein kinase inhibitors and proteasome inhibitors. Protein kinase inhibitors can be divided into Bcr-Abl protein kinase inhibitors, epidermal growth factor receptor tyrosine kinase inhibitors, and multiple kinase target inhibitors.^{46–50} Currently, protein kinase inhibitors commonly used in clinical practice include imatinib, dasatinib, gefitinib, erlotinib, sorafenib, and sunitinib (Fig. 1). These drugs all contain aniline structures. Herein, using sorafenib as the lead compound, sorafenib analogues and derivatives with core aniline structures were designed (Fig. 2) and synthesized. The results of *in vitro* and *in vivo* experiments showed that these compounds had good antitumor activities. In the target molecule design process, bioisosteres and the alkyl principle were used to prepare different compounds. The target compounds were synthesized from 2-aminobenzoic acid (**1a**) or 6-methyl-2-aminobenzoic acid (**1b**) by amination and condensation (*N*-alkylation). The synthetic route involved simple operations and mild reaction conditions, and afforded high total yields (Scheme 1).

2. Results and discussion

2.1. Design and synthesis of sorafenib analogues and derivatives

Sorafenib (protein kinase inhibitor) has a novel structure and is used as an antitumor drug against multiple kinase targets. Herein, the design of protein kinase inhibitors was based on sorafenib as the lead compound. A series of novel sorafenib

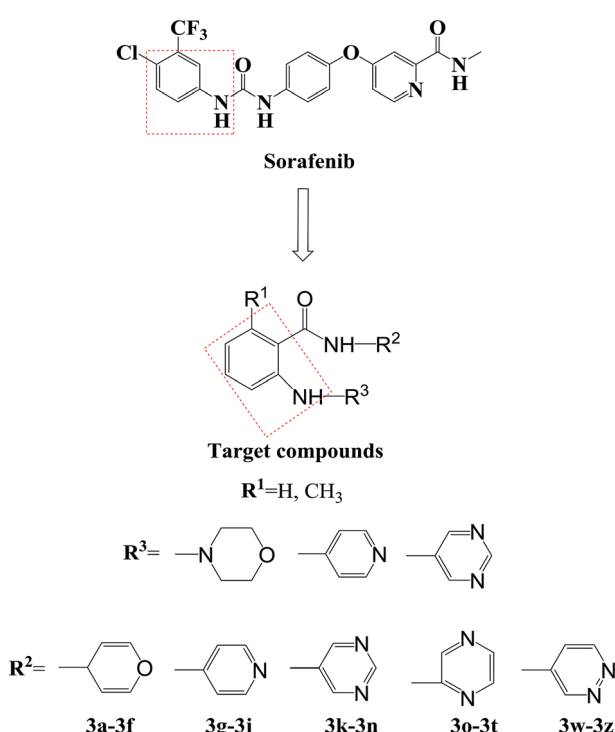
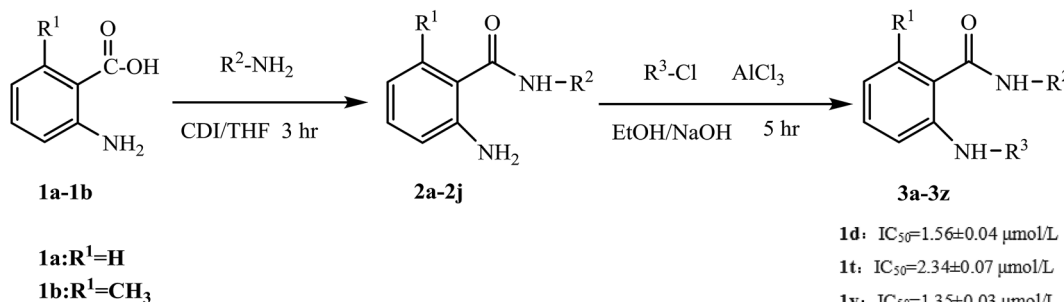


Fig. 2 Design of sorafenib analogues and derivatives.

analogues and derivatives were prepared using bioisosteres and the alkyl principle (Fig. 2). As shown in Fig. 2, the target compounds and sorafenib were found to contain the same aniline structure. According to structure–activity relationship (SAR) studies, this novel series of compounds might have antitumor activities. During structural modification of the lead compound (sorafenib), substituents R^1 , R^2 , and R^3 on the aniline structure were modified. The following substituents were selected and tested: H and CH_3 at R^1 ; pyran, pyridine, pyrimidine, pyrazine, and pyrazidine at R^2 ; and morpholine, pyridine, and pyrimidine at R^3 . These R^1 , R^2 , and R^3 substituents were chosen to alter the physical and chemical properties ($\log P$ and pK_a) of the target compounds and achieve good





Scheme 1 Synthetic route for sorafenib analogues.

biological activity. To prepare the target compounds, we chose a synthesis route that involved simple operations and mild reaction conditions, and afforded high total yields (Scheme 1). As shown in Scheme 1, the target compounds were synthesized by amination and condensation (*N*-alkylation). Compounds 2a–2j were prepared using a general amination method, with 2-aminobenzoic acid (1a) or 6-methyl-2-aminobenzoic acid (1b) as the starting material, tetrahydrofuran (THF) as solvent, and 1,1'-carbonyldiimidazole (CDI) as catalyst under reflux for 3 h to achieve reaction completion. Compounds 3a–3z were prepared using a general condensation (*N*-alkylation) method with AlCl₃ as a catalyst in EtOH/NaOH under reflux for 5 h. The resulting products were characterized by ¹H NMR, ¹³C NMR, HR-ESI-MS, and elemental analysis.

2.2. *In vitro* antitumor activity

Biological activity experiments were based on the MTT assay (a colorimetric assay for assessing cell metabolic activity). For the *in vitro* experiments, human lung cancer cells (H1975 and A549) and cervical cancer cells (Hela) were used as inhibitory targets. The inhibitory activity was measured as the half maximal inhibitory concentration (IC₅₀). Sorafenib and sunitinib were used as positive drugs and DMSO was used as the blank control. The results of the biological activity experiments are shown in Table 1. The data were analyzed by linear regression using statistical software SPSS (version 13.0), with the results showing a linear fit, as shown in Table 1. Compounds 3c, 3d, 3h, 3n, 3r, and 3z showed better inhibitory effects against human cervical cancer cells (Hela), while compounds 3t and 3v showed better inhibitory effects against human lung cancer cells (H1975 and A549). Among these compounds, compound 3d had an inhibitory activity (IC₅₀) of 1.56 ± 0.04 μmol L⁻¹ against Hela cells (human cervical cancer), compound 3t had an IC₅₀ of 2.34 ± 0.07 μmol L⁻¹ against H1975 (human lung cancer), and compound 3v had an IC₅₀ of 1.35 ± 0.03 μmol L⁻¹ against A549 (human lung cancer). As shown in Table 1, these compounds showed good antitumor activity *in vitro*. Compounds 3d and 3r showed better biological activity than positive control sunitinib (IC₅₀ = 2.06 ± 0.34 μmol L⁻¹) against Hela cells, compound 3t showed better biological activity than positive control sorafenib (IC₅₀ = 4.20 ± 0.21 μmol L⁻¹) against H1975 cells, and compound 3v showed similar biological activity to positive control sunitinib (IC₅₀ = 1.05 ± 0.04 μmol L⁻¹) against A549 cells.

2.3. *In vivo* antitumor activity

In vivo antitumor test results are the most important indicators in evaluating the effectiveness of candidate antitumor compounds. *In vivo* experiments were conducted to evaluate the inhibitory effect and intensity of the compounds on the growth of xenograft tumors in nude mice with human carcinoma. During the experiment, human lung cancer (A549) and human cervical cancer (Hela) were inoculated under the right armpit of nude mice. After tumor growth to a certain stage, high (100 mg kg⁻¹ d⁻¹), medium (50 mg kg⁻¹ d⁻¹), and low (10 mg kg⁻¹ d⁻¹) doses of compounds 3c, 3d, 3h, 3n, 3r, 3t, 3v, and 3z were administered (Table 2). Data were analyzed by

Table 1 Inhibitory activity of compounds *in vitro*

Compounds	IC ₅₀ ^a (μmol L ⁻¹) ± SD		
	Hela	A549	H1975
3a	10.20 ± 0.88	12.40 ± 1.20	11.13 ± 1.11
3b	7.02 ± 0.85	10.31 ± 1.00	8.90 ± 0.96
3c	2.01 ± 0.11	25.33 ± 2.05	43.12 ± 3.22
3d	1.56 ± 0.04	20.46 ± 2.20	40.39 ± 2.11
3e	34.78 ± 1.55	12.66 ± 1.03	10.18 ± 1.06
3f	30.69 ± 1.33	10.23 ± 1.09	9.45 ± 0.55
3g	3.08 ± 0.011	10.26 ± 0.65	8.02 ± 0.36
3h	2.07 ± 0.33	7.45 ± 0.45	6.96 ± 0.66
3i	12.67 ± 0.89	56.09 ± 3.00	45.99 ± 2.98
3j	10.33 ± 1.09	54.37 ± 2.16	43.56 ± 3.11
3k	56.88 ± 3.12	4.60 ± 0.45	4.33 ± 0.24
3l	54.70 ± 4.00	3.04 ± 0.73	2.66 ± 0.29
3m	4.04 ± 0.34	24.67 ± 2.23	13.56 ± 1.32
3n	2.54 ± 0.23	20.45 ± 2.10	11.34 ± 1.34
3o	12.45 ± 1.32	15.67 ± 1.58	20.49 ± 1.99
3p	10.45 ± 0.78	13.55 ± 2.10	18.48 ± 2.09
3q	4.22 ± 0.26	23.47 ± 3.12	26.68 ± 2.11
3r	1.90 ± 0.10	19.55 ± 3.10	23.40 ± 2.89
3s	18.34 ± 2.04	4.45 ± 0.21	4.36 ± 0.15
3t	16.23 ± 1.23	3.78 ± 0.21	2.34 ± 0.11
3u	15.04 ± 1.45	2.44 ± 0.14	4.22 ± 0.22
3v	13.58 ± 1.67	1.35 ± 0.02	2.67 ± 0.12
3w	25.55 ± 2.55	13.33 ± 1.89	12.29 ± 2.00
3x	23.68 ± 3.11	10.29 ± 0.90	10.04 ± 0.89
3y	3.46 ± 0.09	46.33 ± 3.11	56.48 ± 4.66
3z	2.11 ± 0.23	44.60 ± 4.21	54.69 ± 5.10
Sorafenib	6.02 ± 0.21	2.10 ± 0.10	4.20 ± 0.21
Sunitinib	2.06 ± 0.34	1.05 ± 0.04	16.02 ± 0.85
DMSO	None	None	None

^a IC₅₀ values are displayed as means ± standard deviations, n ≥ 8.



Table 2 Inhibitory activity of compounds *in vivo*

Compounds	Doses (mg kg ⁻¹ d ⁻¹)	T/C ^a (%)		LD ₅₀ ± SD ^b (mg kg ⁻¹)
		Hela	A549	
3c	10	4.78 ± 0.13	56.78 ± 3.21	2781.2 ± 3.2
	50	1.92 ± 0.09	43.11 ± 3.45	
	100	0.25 ± 0.13	17.23 ± 1.39	
3d	10	3.56 ± 0.08	45.91 ± 3.56	2692.1 ± 4.3
	50	1.26 ± 0.05	37.80 ± 1.34	
	100	0.03 ± 0.01	13.22 ± 1.06	
3h	10	5.11 ± 0.87	38.90 ± 3.10	2469.3 ± 2.8
	50	2.67 ± 0.06	23.53 ± 1.01	
	100	0.30 ± 0.02	9.21 ± 1.31	
3n	10	5.89 ± 0.23	83.26 ± 5.23	1823.2 ± 4.1
	50	2.90 ± 0.10	58.21 ± 3.34	
	100	0.45 ± 0.07	38.33 ± 2.11	
3r	10	4.11 ± 0.19	76.22 ± 4.62	2236.7 ± 3.1
	50	1.87 ± 0.08	52.17 ± 3.12	
	100	0.09 ± 0.01	30.32 ± 3.18	
3t	10	69.45 ± 4.32	5.78 ± 0.56	1803.7 ± 2.3
	50	40.23 ± 2.39	2.26 ± 0.34	
	100	10.12 ± 1.01	0.23 ± 0.02	
3v	10	42.34 ± 3.43	5.38 ± 0.67	2013.5 ± 2.2
	50	36.45 ± 1.22	2.11 ± 0.05	
	100	6.55 ± 0.33	0.11 ± 0.03	
3z	10	6.35 ± 0.56	71.31 ± 3.42	1749.1 ± 3.2
	50	2.93 ± 0.08	58.51 ± 2.32	
	100	0.31 ± 0.01	41.12 ± 1.23	
Sorafenib	50	9.56 ± 1.05	3.11 ± 0.23	2210.5 ± 2.3
Sunitinib	50	2.89 ± 0.02	2.21 ± 0.15	2331.2 ± 2.1
DMSO	50	100	100	

^a T/C values are displayed as means ± standard deviations, *n* ≥ 8. ^b LD₅₀ values are displayed as means ± standard deviations, *n* ≥ 8.

linear regression using statistical software SPSS (version 13.0), with the results of data analysis showing a linear fit. As shown in Table 2, the data showed that these compounds had good antitumor effects *in vivo* and showed low relative tumor proliferation rates (T/C, %). Most of the compounds were effective at high, medium, and low doses (T/C > 40% was ineffective and T/C ≤ 40% was effective). As shown in Table 2, compounds **3c**, **3d**, **3h**, **3n**, **3r**, and **3z** showed general inhibitory activities at low doses (10 mg kg⁻¹ d⁻¹) against Hela cells. However, at medium doses (50 mg kg⁻¹ d⁻¹) or high doses (100 mg kg⁻¹ d⁻¹), their inhibitory activities were significantly increased above those of positive controls sorafenib and sunitinib. Compounds **3t** and **3v** showed general inhibitory activity at low doses (10 mg kg⁻¹ d⁻¹) against A549 cells, but better activities than positive controls sorafenib and sunitinib at medium (50 mg kg⁻¹ d⁻¹) and high doses (100 mg kg⁻¹ d⁻¹). Therefore good inhibitory activities were obtained at medium doses and high doses against Hela and A549 cells *in vivo*. We also studied the acute toxicity of these target compounds *in vivo* (Table 2), which found that target compounds **3c**, **3d**, **3h**, **3n**, **3r**, **3t**, **3v**, and **3z** had low acute toxicity.

3. Conclusions

We have reported the design, synthesis, and evaluation of a series of novel sorafenib analogues and derivatives as

tumor inhibitors. Using sorafenib as the lead compound, various compounds were designed and prepared using bioisosteres and the alkyl principle. The target compounds were synthesized from 2-aminobenzoic acid (**1a**) or 6-methyl-2-aminobenzoic acid (**1b**) by amination and condensation (*N*-alkylation). This synthetic route involved simple operations and mild reaction conditions, and afforded high total yields. *In vitro* activity results showed that compounds **3c**, **3d**, **3h**, **3n**, **3r**, and **3z** had good inhibitory effects on human cervical cancer cells (Hela), and that compounds **3t** and **3v** had good inhibitory effects on human lung cancer cells (H1975 and A549). Among these compounds, compound **3d** had an inhibitory activity (IC₅₀) of 1.56 ± 0.04 μmol L⁻¹ against Hela cells (human cervical cancer), compound **3t** had an IC₅₀ of 2.34 ± 0.07 μmol L⁻¹ against H1975 cells (human lung cancer), and compound **3v** had an IC₅₀ of 1.35 ± 0.03 μmol L⁻¹ against A549 cells (human lung cancer). *In vivo* activity results showed that these compounds had good antitumor effects and low acute toxicity.

4. Experimental

4.1. Chemistry

4.1.1. Materials and general methods. Reagents were purchased and used without further purification. Nuclear magnetic resonance (NMR) spectroscopy was performed on



a Bruker AMX-400 (TMS as internal standard). Mass spectrometry was performed on a Agilent 6460 spectrometer. HPLC analysis of all final biologically tested compounds was performed on an Agilent 1260 Series HPLC system. Purity was determined using reversed-phase HPLC and was $\geq 99\%$ for all biologically tested compounds.

4.1.2. Synthesis of compounds 2a–2j. The synthesis of compound **2a** is described here as an example. To 1,1-carbonylidimidazole (CDI; 16.20 g, 0.10 mol) dissolved in THF (30 mL) at around 10 °C was added 4-amino-4*H*-pyran (8.20 g, 0.10 mol), and the mixture was stirred continuously for 30 min. Next, 2-aminobenzoic acid (**1a**, 13.70 g, 0.10 mol) dissolved in THF (100 mL) in a 250 mL round bottom flask was added dropwise to the reaction mixture at 10 °C, followed by reflux for 3 h. After reaction completion, the mixture was allowed to cool and the precipitated solid was filtered, washed, and dried *in vacuo* to afford crude product 2-amino-*N*-(4*H*-pyran-4-yl)benzamide (**2a**). Crude **2a** was recrystallized from acetone, filtered, and dried *in vacuo* to afford pure **2a** as a white crystalline solid. This general procedure was used for the synthesis of compounds **2b–2j**.

4.1.3. Synthesis of compounds 3a–3z. The synthesis of compound **3a** is described here as an example. To compound **2a** (21.10 g, 0.10 mol) in a 250 mL round bottom flask was added anhydrous ethanol (100 mL) and anhydrous aluminum trichloride (13.30 g, 0.01 mol). Under constant pressure conditions, 4-chloromorpholine (12.15 g, 0.10 mol) was added dropwise using a dropping funnel, and then the reaction was refluxed for 5 h. After reaction completion, the mixture was filtered while still hot and ethanol was removed from the filtrate under normal pressure. The mixture was dried *in vacuo* to afford crude product **3a**. Crude **3a** was recrystallized from ethanol (volume fraction, 60%), filtered, and dried *in vacuo* to afford pure **3a** as a white crystalline solid. This general procedure was used for the synthesis of compounds **3b–3z**.

2-(Morpholinoamino)-*N*-(4*H*-pyran-4-yl)benzamide (3a**).** 84.8% yield; mp 145–146 °C; ¹H NMR (300 MHz, CDCl₃) δ : 9.18 (s, 1H, –NH–), 7.69 (m, 1H, Ph-H), 7.50 (m, 1H, Ph-H), 7.08 (m, 1H, Ph-H), 6.78 (m, 1H, Ph-H), 6.17 (d, *J* = 8.4 Hz, 2H, C=CH-O), 4.76 (m, 1H, –CH–), 4.63 (m, 2H, –CH=C), 3.65 (m, 4H, C–CH₂–O), 3.00 (m, 4H, –CH₂–C); ¹³C NMR (75 MHz, CDCl₃) δ : 167.8, 141.0, 140.1, 132.6, 128.0, 119.2, 114.8, 112.1, 104.1, 65.5, 58.4, 51.1; HR-ESI-MS *m/z*: calcd for C₁₆H₁₉N₃O₃ ([M + H]⁺), 301.3503; found, 301.3501. Anal. calcd for C₁₆H₁₉N₃O₃: C, 63.77; H, 6.36; N, 13.94; O, 15.93; found: C, 63.76; H, 6.37; N, 13.93; O, 15.94%.

2-Methyl-6-(morpholinoamino)-*N*-(4*H*-pyran-4-yl)benzamide (3b**).** 89.2% yield; mp 153–156 °C; ¹H NMR (300 MHz, CDCl₃) δ : 9.18 (s, 1H, –NH–), 7.36 (m, 1H, Ph-H), 6.98 (m, 1H, Ph-H), 6.69 (m, 1H, Ph-H), 6.17 (d, *J* = 8.4 Hz, 2H, C=CH-O), 4.76 (m, 1H, –CH–), 4.63 (m, 2H, –CH=C), 3.65 (m, 4H, C–CH₂–O), 3.00 (m, 4H, –CH₂–C), 2.48 (s, 3H, –CH₃); ¹³C NMR (75 MHz, CDCl₃) δ : 167.8, 140.9, 140.1, 137.7, 132.5, 121.9, 117.7, 104.1, 65.5, 58.4, 51.1; HR-ESI-MS *m/z*: calcd for C₁₇H₂₁N₃O₃ ([M + H]⁺), 315.3701; found, 315.1583; anal. calcd for C₁₇H₂₁N₃O₃: C, 64.74; H, 6.71; N, 13.32; O, 15.22; found: C, 64.73; H, 6.72; N, 13.33; O, 15.21%.

***N*-(4*H*-Pyran-4-yl)-2-(pyridin-4-ylamino)benzamide (**3c**).** 90.1% yield; mp 173–174 °C; ¹H NMR (300 MHz, CDCl₃) δ : 11.02 (s, 1H, –NH–N), 9.18 (s, 1H, –NH–), 8.46 (m, 2H, –CH=N), 8.39 (m, 1H, Ph-H), 7.73 (m, 1H, Ph-H), 7.66 (m, 1H, Ph-H), 6.99 (m, 1H, Ph-H), 6.99 (m, 2H, C=CH–), 6.17 (d, *J* = 8.4 Hz, 2H, C=CH-O), 4.76 (m, 1H, –CH–), 4.63 (m, 2H, –CH=C); ¹³C NMR (75 MHz, CDCl₃) δ : 167.8, 155.3, 151.9, 150.2, 140.1, 132.9, 128.3, 118.8, 117.9, 116.4, 109.0, 104.1, 51.1; HR-ESI-MS *m/z*: calcd for C₁₇H₁₅N₃O₂ ([M + H]⁺), 293.3301; found, 293.1164; anal. calcd for C₁₇H₁₅N₃O₂: C, 69.61; H, 5.15; N, 14.33; O, 10.91; found: C, 69.60; H, 5.17; N, 14.32; O, 10.91%.

2-Methyl-*N*-(4*H*-pyran-4-yl)-6-(pyridin-4-ylamino)benzamide (3d**).** 92.5% yield; mp 182–185 °C; ¹H NMR (300 MHz, CDCl₃) δ : 11.02 (s, 1H, –NH–N), 9.18 (s, 1H, –NH–), 8.46 (m, 2H, –CH=N), 8.29 (m, 1H, Ph-H), 7.40 (m, 1H, Ph-H), 6.99 (m, 2H, C=CH–), 6.90 (m, 1H, Ph-H), 6.17 (d, *J* = 8.4 Hz, 2H, C=CH-O), 4.76 (m, 1H, –CH–), 4.63 (m, 2H, –CH=C), 2.48 (s, 3H, –CH₃); ¹³C NMR (75 MHz, CDCl₃) δ : 167.8, 155.3, 150.2, 143.8, 143.1, 140.1, 138.0, 121.5, 120.8, 113.4, 109.0, 104.1, 51.1, 18.1; HR-ESI-MS *m/z*: calcd for C₁₈H₁₇N₃O₂ ([M + H]⁺), 307.3505; found, 307.1320; anal. calcd for C₁₈H₁₇N₃O₂: C, 70.34; H, 5.58; N, 13.67; O, 10.41; found: C, 70.35; H, 5.59; N, 13.66; O, 10.40%.

***N*-(4*H*-Pyran-4-yl)-2-(pyrimidin-5-ylamino)benzamide (**3e**).** 93.4% yield; mp 201–203 °C; ¹H NMR (300 MHz, CDCl₃) δ : 9.23 (s, 1H, –NH–C), 9.18 (s, 1H, –NH–C), 8.90 (s, 1H, N=CH–N), 8.50 (s, 1H, –CH=N), 8.39 (m, 1H, Ph-H), 7.73 (m, 1H, Ph-H), 7.66 (m, 1H, Ph-H), 6.99 (m, 1H, Ph-H), 6.17 (d, *J* = 8.4 Hz, 2H, C=CH-O), 4.76 (m, 1H, –CH–), 4.63 (m, 2H, –CH=C); ¹³C NMR (75 MHz, CDCl₃) δ : 167.8, 151.9, 147.4, 143.7, 142.9, 140.1, 132.9, 128.3, 118.8, 117.9, 116.4, 104.1, 51.1; HR-ESI-MS *m/z*: calcd for C₁₆H₁₄N₄O₂ ([M + H]⁺), 294.3101; found, 294.1117; anal. calcd for C₁₆H₁₄N₄O₂: C, 65.30; H, 4.79; N, 19.04; O, 10.87; found: C, 65.31; H, 4.79; N, 19.03; O, 10.87%.

2-Methyl-*N*-(4*H*-pyran-4-yl)-6-(pyrimidin-5-ylamino)benzamide (3f**).** 94.0% yield, mp 222–223 °C; ¹H NMR (300 MHz, CDCl₃) δ : 9.23 (s, 1H, –NH–C), 9.18 (s, 1H, –NH–C), 8.90 (s, 1H, N=CH–N), 8.50 (s, 1H, –CH=N), 8.29 (m, 1H, Ph-H), 7.40 (m, 1H, Ph-H), 6.90 (m, 1H, Ph-H), 6.17 (d, *J* = 8.4 Hz, 2H, C=CH-O), 4.76 (m, 1H, –CH–), 4.63 (m, 2H, –CH=C), 2.48 (s, 3H, –CH₃); ¹³C NMR (75 MHz, CDCl₃) δ : 167.8, 147.4, 143.8, 143.7, 143.1, 140.1, 138.0, 121.5, 120.8, 113.4, 104.1, 51.1, 18.1; HR-ESI-MS *m/z*: calcd for C₁₇H₁₆N₄O₂ ([M + H]⁺), 308.3411; found, 308.1273; anal. calcd for C₁₇H₁₆N₄O₂: C, 66.22; H, 5.23; N, 18.17; O, 10.38; found: C, 66.23; H, 5.22; N, 18.18; O, 10.37%.

2-(Morpholinoamino)-*N*-(pyridin-4-yl)benzamide (3g**).** 88.4% yield; mp 168–170 °C; ¹H NMR (300 MHz, CDCl₃) δ : 10.35 (s, 1H, –NH–N), 10.22 (s, 1H, –NH–), 8.46 (d, *J* = 7.4 Hz, 2H, –CH=N), 7.69 (m, 1H, Ph-H), 7.50 (m, 1H, Ph-H), 7.36 (d, *J* = 7.2 Hz, 2H, –CH=C), 7.08 (m, 1H, Ph-H), 3.65 (m, 4H, C–CH₂–O), 3.00 (m, 4H, –CH₂–C); ¹³C NMR (75 MHz, CDCl₃) δ : 167.5, 155.3, 150.2, 141.0, 132.6, 128.0, 119.2, 114.8, 112.1, 109.0, 65.5, 58.4; HR-ESI-MS *m/z*: calcd for C₁₆H₁₄N₄O₂ ([M + H]⁺), 294.3111; found, 294.1116; anal. calcd for C₁₆H₁₄N₄O₂: C, 65.30; H, 4.79; N, 19.04; O, 10.87; found: C, 65.31; H, 4.78; N, 19.04; O, 10.87%

2-Methyl-6-(morpholinoamino)-*N*-(pyridin-4-yl)benzamide (3h**).** 90.2% yield; mp 177–178 °C; ¹H NMR (300 MHz, CDCl₃) δ : 10.35



(s, 1H, -NH-N), 10.22 (s, 1H, -NH-), 8.46 (d, J = 7.4 Hz, 2H, -CH=N), 7.36 (d, J = 7.2 Hz, 2H, -CH=C), 7.36 (m, 1H, Ph-H), 6.98 (m, 1H, Ph-H), 6.69 (m, 1H, Ph-H), 3.65 (m, 4H, C-CH₂-O), 3.00 (m, 4H, -CH₂-C), 2.48 (s, 3H, -CH₃); ¹³C NMR (75 MHz, CDCl₃) δ : 164.7, 155.3, 150.2, 140.9, 137.7, 132.5, 121.9, 117.7, 109.1, 109.0, 65.5, 58.4, 18.1; HR-ESI-MS *m/z*: calcd for C₁₇H₁₆N₄O₂ ([M + H]⁺), 308.3400; found, 308.1273; anal. calcd for C₁₇H₁₆N₄O₂: C, 66.22; H, 5.23; N, 18.17; O, 10.38; found: C, 66.23; H, 5.24; N, 18.15; O, 10.38%.

N-(Pyridin-4-yl)-2-(pyrimidin-5-ylamino)benzamide (3i). 92.1% yield; mp 188–190 °C; ¹H NMR (300 MHz, CDCl₃) δ : 10.22 (s, 1H, -NH-N), 9.23 (s, 1H, -NH-), 8.90 (s, 1H, -N-CH-), 8.50 (s, 2H, -CH=N), 8.46 (d, J = 7.4 Hz, 2H, -CH=N), 8.39 (m, 1H, Ph-H), 7.73 (m, 1H, Ph-H), 7.66 (m, 1H, Ph-H), 7.36 (d, J = 7.2 Hz, 2H, -CH=C), 6.99 (m, 1H, Ph-H); ¹³C NMR (75 MHz, CDCl₃) δ : 167.5, 155.3, 151.9, 150.2, 147.4, 143.7, 142.9, 132.9, 128.3, 118.8, 117.9, 116.4, 109.0; HR-ESI-MS *m/z*: calcd for C₁₆H₁₃N₅O ([M + H]⁺), 291.3100; found, 291.1120; anal. calcd for C₁₆H₁₃N₅O: C, 65.97; H, 4.50; N, 24.04; O, 5.49; found: C, 65.97; H, 4.51; N, 24.04; O, 5.48%.

2-Methyl-N-(pyridin-4-yl)-6-(pyrimidin-5-ylamino)benzamide (3j). 92.9% yield; mp 201–204 °C; ¹H NMR (300 MHz, CDCl₃) δ : 10.22 (s, 1H, -NH-N), 9.23 (s, 1H, -NH-), 8.90 (s, 1H, -N-CH-), 8.50 (s, 2H, -CH=N), 8.46 (d, J = 7.4 Hz, 2H, -CH=N), 8.29 (m, 1H, Ph-H), 7.40 (d, J = 7.2 Hz, 2H, -CH=C), 7.36 (d, J = 7.2 Hz, 2H, -CH=C), 6.90 (m, 1H, Ph-H); 2.48 (s, 3H, -CH₃); ¹³C NMR (75 MHz, CDCl₃) δ : 164.7, 155.3, 150.2, 147.4, 143.8, 143.7, 143.1, 142.9, 138.0, 121.5, 120.8, 113.4, 109.0, 18.1; HR-ESI-MS *m/z*: calcd for C₁₇H₁₅N₅O ([M + H]⁺), 305.3401; found, 305.1277; anal. calcd for C₁₇H₁₅N₅O: C, 66.87; H, 4.95; N, 22.94; O, 5.24; found: C, 66.88; H, 4.95; N, 22.94; O, 5.23%.

2-(Morpholinoamino)-N-(pyrimidin-5-yl)benzamide (3k). 87.1% yield; mp 178–180 °C; ¹H NMR (300 MHz, CDCl₃) δ : 10.35 (s, 1H, -NH-N), 10.22 (s, 1H, -NH-), 9.21 (s, 2H, -CH=N), 9.10 (s, 1H, -N=CH-), 7.69 (m, 1H, Ph-H), 7.50 (m, 1H, Ph-H), 7.08 (m, 1H, Ph-H), 3.65 (m, 4H, C-CH₂-O), 3.00 (m, 4H, -CH₂-C); ¹³C NMR (75 MHz, CDCl₃) δ : 167.5, 147.4, 143.7, 141.1, 141.0, 132.6, 128.0, 119.2, 114.8, 112.1, 65.5, 58.4; HR-ESI-MS *m/z*: calcd for C₁₅H₁₇N₅O₂ ([M + H]⁺), 299.3301; found, 299.1382; anal. calcd for C₁₅H₁₇N₅O₂: C, 60.19; H, 5.72; N, 23.40; O, 10.69; found: C, 60.19; H, 5.73; N, 23.40; O, 10.68%.

2-Methyl-6-(morpholinoamino)-N-(pyrimidin-5-yl)benzamide (3l). 89.0% yield; mp 192–194 °C; ¹H NMR (300 MHz, CDCl₃) δ : 10.35 (s, 1H, -NH-N), 10.22 (s, 1H, -NH-), 9.21 (s, 2H, -CH=N), 9.10 (s, 1H, -N=CH-), 7.36 (m, 1H, Ph-H), 6.98 (m, 1H, Ph-H), 6.69 (m, 1H, Ph-H), 3.65 (m, 4H, C-CH₂-O), 3.00 (m, 4H, -CH₂-C), 2.48 (s, 3H, -CH₃); ¹³C NMR (75 MHz, CDCl₃) δ : 164.7, 147.4, 143.7, 141.1, 140.9, 137.7, 132.5, 121.9, 117.7, 109.1, 65.5, 58.4, 18.1; HR-ESI-MS *m/z*: calcd for C₁₆H₁₉N₅O₂ ([M + H]⁺), 313.3602; found, 313.1539; anal. calcd for C₁₆H₁₉N₅O₂: C, 61.33; H, 6.11; N, 22.35; O, 10.21; found: C, 61.35; H, 6.10; N, 22.35; O, 10.20%.

2-(Pyridin-4-ylamino)-N-(pyrimidin-5-yl)benzamide (3m). 90.2% yield; mp 192–193 °C; ¹H NMR (300 MHz, CDCl₃) δ : 11.02 (s, 1H, -NH-N), 10.21 (s, 1H, -NH-), 9.21 (s, 2H, -CH=N), 9.10 (s, 1H, -N=CH-), 8.46 (m, 2H, -CH-N), 8.39 (m, 1H, Ph-H), 7.73 (m, 1H, Ph-H), 7.66 (m, 1H, Ph-H), 6.99 (m, 1H, Ph-H), 6.99 (m, 2H,

-C-CH-); ¹³C NMR (75 MHz, CDCl₃) δ : 167.5, 155.3, 151.9, 150.2, 147.4, 143.7, 141.1, 132.9, 128.3, 118.8, 117.9, 116.4, 109.0; HR-ESI-MS *m/z*: calcd for C₁₆H₁₃N₅O ([M + H]⁺), 291.3112; found, 291.1120; anal. calcd for C₁₆H₁₃N₅O: C, 65.97; H, 4.50; N, 24.04; O, 5.49; found: C, 65.98; H, 4.51; N, 24.03; O, 5.48%.

2-Methyl-6-(pyridin-4-ylamino)-N-(pyrimidin-5-yl)benzamide (3n). 93.1% yield; mp 201–202 °C; ¹H NMR (300 MHz, CDCl₃) δ : 11.02 (s, 1H, -NH-N), 10.21 (s, 1H, -NH-), 9.21 (s, 2H, -CH=N), 9.10 (s, 1H, -N=CH-), 8.46 (m, 2H, -CH-N), 8.29 (m, 1H, Ph-H), 7.40 (m, 1H, Ph-H), 6.99 (m, 2H, -C-CH-), 6.90 (m, 1H, Ph-H), 2.48 (s, 3H, -CH₃); ¹³C NMR (75 MHz, CDCl₃) δ : 164.7, 155.3, 150.2, 147.4, 143.8, 143.7, 143.1, 141.1, 138.0, 121.5, 120.8, 113.4, 109.0, 18.1; HR-ESI-MS *m/z*: calcd for C₁₇H₁₅N₅O ([M + H]⁺), 305.3411; found, 305.1276; anal. calcd for C₁₇H₁₅N₅O: C, 66.87; H, 4.95; N, 22.94; O, 5.24; found: C, 66.88; H, 4.94; N, 22.93; O, 5.25%.

2-(Morpholinoamino)-N-(pyrazin-2-yl)benzamide (3o). 86.3% yield; mp 181–183 °C; ¹H NMR (300 MHz, CDCl₃) δ : 12.32 (s, 1H, -NH-N), 11.17 (s, 1H, -NH-), 8.59 (s, 1H, -CH-N), 8.40 (s, 1H, -N=CH-), 8.35 (s, 1H, -N=CH-), 7.69 (m, 1H, Ph-H), 7.50 (m, 1H, Ph-H), 7.08 (m, 1H, Ph-H), 6.78 (m, 1H, Ph-H), 3.65 (m, 4H, C-CH₂-O), 3.00 (m, 4H, -CH₂-C); ¹³C NMR (75 MHz, CDCl₃) δ : 164.7, 149.7, 141.8, 139.5, 137.4, 136.1, 132.6, 128.0, 119.2, 114.8, 112.1, 65.5, 58.4; HR-ESI-MS *m/z*: calcd for C₁₅H₁₇N₅O₂ ([M + H]⁺), 299.3312; found, 299.1382; anal. calcd for C₁₅H₁₇N₅O₂: C, 60.19; H, 5.72; N, 23.40; O, 10.69; found: C, 60.19; H, 5.73; N, 23.41; O, 10.67%.

2-Methyl-6-(morpholinoamino)-N-(pyrazin-2-yl)benzamide (3p). 89.1% yield; mp 194–196 °C; ¹H NMR (300 MHz, CDCl₃) δ : 12.32 (s, 1H, -NH-N), 11.17 (s, 1H, -NH-), 8.59 (s, 1H, -CH-N), 8.40 (s, 1H, -N=CH-), 8.35 (s, 1H, -N=CH-), 7.36 (m, 1H, Ph-H), 6.98 (m, 1H, Ph-H), 6.69 (m, 1H, Ph-H), 3.65 (m, 4H, C-CH₂-O), 3.00 (m, 4H, -CH₂-C), 2.48 (s, 3H, -CH₃); ¹³C NMR (75 MHz, CDCl₃) δ : 164.7, 149.7, 140.9, 139.5, 137.4, 137.7, 137.4, 136.1, 132.5, 121.9, 117.7, 109.1, 65.5, 58.4; HR-ESI-MS *m/z*: calcd for C₁₆H₁₉N₅O₂ ([M + H]⁺), 313.3611; found, 313.1538; anal. calcd for C₁₆H₁₉N₅O₂: C, 61.33; H, 6.11; N, 22.35; O, 10.21; found: C, 61.34; H, 6.10; N, 22.35; O, 10.21%.

N-(Pyrazin-2-yl)-2-(pyridin-4-ylamino)benzamide (3q). 86.3% yield; mp 196–198 °C; ¹H NMR (300 MHz, CDCl₃) δ : 11.17 (s, 1H, -NH-N), 11.02 (s, 1H, -NH-), 8.59 (s, 1H, -CH-N), 8.46 (m, 2H, -CH-N), 8.40 (s, 1H, -N=CH-), 8.39 (m, 1H, Ph-H), 8.35 (s, 1H, -N=CH-), 7.73 (m, 1H, Ph-H), 7.66 (m, 1H, Ph-H), 6.99 (m, 1H, Ph-H), 6.99 (m, 2H, -C-CH-); ¹³C NMR (75 MHz, CDCl₃) δ : 164.7, 155.3, 151.9, 150.2, 149.7, 139.5, 137.4, 136.1, 132.9, 128.3, 118.8, 117.9, 116.4, 109.0; HR-ESI-MS *m/z*: calcd for C₁₆H₁₃N₅O ([M + H]⁺), 291.3122; found, 291.1120; anal. calcd for C₁₆H₁₃N₅O: C, 65.97; H, 4.50; N, 24.04; O, 5.49; found: C, 65.98; H, 4.50; N, 24.05; O, 5.47%.

2-Methyl-N-(pyrazin-2-yl)-6-(pyridin-4-ylamino)benzamide (3r). 88.4% yield; mp 210–212 °C; ¹H NMR (300 MHz, CDCl₃) δ : 11.17 (s, 1H, -NH-N), 11.02 (s, 1H, -NH-), 8.59 (s, 1H, -CH-N), 8.46 (m, 2H, -CH-N), 8.40 (s, 1H, -N=CH-), 8.29 (m, 1H, Ph-H), 8.35 (s, 1H, -N=CH-), 7.40 (m, 1H, Ph-H), 6.99 (m, 2H, -C-CH-); ¹³C NMR (75 MHz, CDCl₃) δ : 164.7, 155.3, 150.2, 149.7, 143.8, 143.1, 139.5, 138.0, 137.4, 136.1, 121.5, 121.5, 120.8, 113.4, 109.0, 18.1; HR-ESI-MS *m/z*: calcd for C₁₇H₁₅N₅O₂ ([M + H]⁺), 313.3602; found, 313.1539; anal. calcd for C₁₇H₁₅N₅O₂: C, 66.87; H, 4.95; N, 22.35; O, 10.21; found: C, 66.88; H, 4.94; N, 22.33; O, 10.21%.



calcd for $C_{17}H_{15}N_5O$ ($[M + H]^+$), 305.3402; found, 305.1277; anal. calcd for $C_{17}H_{15}N_5O$: C, 66.87; H, 4.95; N, 22.94; O, 5.24; found: C, 66.88; H, 4.95; N, 22.93; O, 5.24%.

N-(Pyrazin-2-yl)-2-(pyrimidin-5-ylamino)benzamide (3s). 90.2% yield, mp 212–214 °C; 1H NMR (300 MHz, $CDCl_3$) δ : 11.17 (s, 1H, –NH–N), 9.20 (s, 1H, –NH–), 8.90 (s, 1H, –N–CH–), 8.59 (s, 1H, –CH–N), 8.50 (s, 2H, –CH==N), 8.40 (s, 1H, –N=CH–), 8.39 (m, 1H, Ph–H), 8.35 (s, 1H, –N=CH–), 7.73 (m, 1H, Ph–H), 7.66 (m, 1H, Ph–H), 6.99 (m, 1H, Ph–H); ^{13}C NMR (75 MHz, $CDCl_3$) δ : 164.7, 151.9, 149.7, 147.4, 143.7, 142.9, 139.5, 137.4, 136.1, 132.9, 128.3, 118.8, 117.9, 116.4; HR-ESI-MS m/z : calcd for $C_{15}H_{12}N_6O$ ($[M + H]^+$), 292.3002; found, 292.1072; anal. calcd for $C_{15}H_{12}N_6O$: C, 61.64; H, 4.14; N, 28.75; O, 5.47; found: C, 61.65; H, 4.15; N, 28.74; O, 5.46%.

2-Methyl-N-(pyrazin-2-yl)-6-(pyrimidin-5-ylamino)benzamide (3t). 91.4% yield; mp 222–224 °C; 1H NMR (300 MHz, $CDCl_3$) δ : 11.17 (s, 1H, –NH–N), 9.20 (s, 1H, –NH–), 8.90 (s, 1H, –N–CH–), 8.59 (s, 1H, –CH–N), 8.50 (s, 2H, –CH==N), 8.40 (s, 1H, –N=CH–), 8.35 (s, 1H, –N=CH–), 8.29 (m, 1H, Ph–H), 7.40 (m, 1H, Ph–H), 6.90 (m, 1H, Ph–H), 2.48 (s, 3H, –CH₃); ^{13}C NMR (75 MHz, $CDCl_3$) δ : 164.7, 149.7, 147.4, 143.8, 143.7, 143.1, 142.9, 139.5, 138.0, 137.4, 136.1, 121.5, 120.8, 113.4, 18.1; HR-ESI-MS m/z : calcd for $C_{16}H_{14}N_6O$ ($[M + H]^+$), 306.3302; found, 306.1229; anal. calcd for $C_{16}H_{14}N_6O$: C, 62.74; H, 4.61; N, 27.43; O, 5.22; found: C, 62.75; H, 4.61; N, 26.43; O, 5.22%.

2-(Morpholinoamino)-N-(pyridazin-4-yl)benzamide (3u). 87.3% yield; mp 167–168 °C; 1H NMR (300 MHz, $CDCl_3$) δ : 11.20 (s, 1H, –NH–N), 10.37 (s, 1H, –NH–), 9.61 (s, 1H, –CH–N), 9.30 (m, 1H, –CH–N), 8.05 (m, 1H, –C–CH–), 7.69 (m, 1H, Ph–H), 7.50 (m, 1H, Ph–H), 7.08 (m, 1H, Ph–H), 6.78 (m, 1H, Ph–H), 3.65 (m, 4H, C–CH₂–O), 3.00 (m, 4H, –CH₂–C); ^{13}C NMR (75 MHz, $CDCl_3$) δ : 167.5, 150.4, 144.2, 141.0, 139.4, 132.6, 128.0, 119.2, 114.8, 114.2, 112.1, 65.5, 58.4; HR-ESI-MS m/z : calcd for $C_{15}H_{17}N_5O_2$ ($[M + H]^+$), 299.3302; found, 299.1382; anal. calcd for $C_{15}H_{17}N_5O_2$: C, 60.19; H, 5.72; N, 23.40; O, 10.69; found: C, 60.20; H, 5.71; N, 23.39; O, 10.70%.

2-Methyl-6-(morpholinoamino)-N-(pyridazin-4-yl)benzamide (3v). 88.5% yield; mp 182–184 °C; 1H NMR (300 MHz, $CDCl_3$) δ : 11.20 (s, 1H, –NH–N), 10.37 (s, 1H, –NH–), 9.61 (s, 1H, –CH–N), 9.30 (m, 1H, –CH–N), 8.05 (m, 1H, –C–CH–), 7.36 (m, 1H, Ph–H), 6.98 (m, 1H, Ph–H), 6.69 (m, 1H, Ph–H), 3.65 (m, 4H, C–CH₂–O), 3.00 (m, 4H, –CH₂–C), 2.48 (s, 3H, –CH₃); ^{13}C NMR (75 MHz, $CDCl_3$) δ : 164.7, 150.4, 144.2, 140.9, 139.4, 137.7, 132.5, 121.9, 117.7, 114.2, 109.1, 65.5, 58.4, 18.1; HR-ESI-MS m/z : calcd for $C_{16}H_{19}N_5O_2$ ($[M + H]^+$), 313.3611; found, 313.1538; anal. calcd for $C_{16}H_{19}N_5O_2$: C, 61.33; H, 6.11; N, 22.35; O, 10.21; found: C, 61.34; H, 6.12; N, 22.34; O, 10.20%.

N-(Pyridazin-4-yl)-2-(pyridin-4-ylamino)benzamide (3w). 88.5% yield; mp 182–184 °C; 1H NMR (300 MHz, $CDCl_3$) δ : 11.02 (s, 1H, –NH–N), 10.37 (s, 1H, –NH–), 9.61 (s, 1H, –CH–N), 9.30 (m, 1H, –CH–N), 8.46 (m, 2H, –CH–N), 8.39 (m, 1H, Ph–H), 8.05 (m, 1H, –C–CH–), 7.73 (m, 1H, Ph–H), 7.66 (m, 1H, Ph–H), 6.99 (m, 1H, Ph–H), 6.99 (m, 2H, –C–CH–); ^{13}C NMR (75 MHz, $CDCl_3$) δ : 167.5, 155.3, 151.9, 150.4, 150.2, 144.2, 139.4, 132.9, 128.3, 118.8, 117.9, 116.4, 114.2, 109.0; HR-ESI-MS m/z : calcd for $C_{16}H_{13}N_5O$ ($[M + H]^+$), 291.3102; found, 291.1120; anal. calcd for

$C_{16}H_{13}N_5O$: C, 65.97; H, 4.50; N, 24.04; O, 5.49; found: C, 65.98; H, 4.51; N, 24.03; O, 5.48%.

2-Methyl-N-(pyridazin-4-yl)-6-(pyridin-4-ylamino)benzamide (3x). 90.2% yield; mp 193–195 °C; 1H NMR (300 MHz, $CDCl_3$) δ : 11.02 (s, 1H, –NH–N), 10.37 (s, 1H, –NH–), 9.61 (s, 1H, –CH–N), 9.30 (m, 1H, –CH–N), 8.46 (m, 2H, –CH–N), 8.29 (m, 1H, Ph–H), 8.05 (m, 1H, –C–CH–), 7.40 (m, 1H, Ph–H), 6.99 (m, 1H, Ph–H), 6.99 (m, 2H, –C–CH–), 2.48 (s, 3H, –CH₃); ^{13}C NMR (75 MHz, $CDCl_3$) δ : 164.7, 155.3, 150.4, 150.2, 144.2, 143.8, 143.1, 139.4, 138.0, 121.5, 120.8, 114.2, 113.4, 109.0, 18.1; HR-ESI-MS m/z : calcd for $C_{17}H_{15}N_5O$ ($[M + H]^+$), 305.3402; found, 305.1276; anal. calcd for $C_{17}H_{15}N_5O$: C, 66.87; H, 4.95; N, 22.94; O, 5.24; found: C, 66.88; H, 4.95; N, 22.93; O, 5.24%.

N-(Pyridazin-4-yl)-2-(pyrimidin-5-ylamino)benzamide (3y). 91.1% yield; mp 198–200 °C; 1H NMR (300 MHz, $CDCl_3$) δ : 11.02 (s, 1H, –NH–N), 10.37 (s, 1H, –NH–), 9.61 (s, 1H, –CH–N), 9.30 (m, 1H, –CH–N), 8.90 (s, 1H, –N–CH–), 8.50 (s, 2H, –CH==N), 8.39 (m, 1H, Ph–H), 7.73 (m, 1H, Ph–H), 7.66 (m, 1H, Ph–H), 6.99 (m, 1H, Ph–H); ^{13}C NMR (75 MHz, $CDCl_3$) δ : 167.5, 151.9, 150.4, 147.4, 144.2, 143.7, 142.9, 139.4, 132.9, 128.3, 118.8, 117.9, 116.4, 114.2; HR-ESI-MS m/z : calcd for $C_{15}H_{12}N_6O$ ($[M + H]^+$), 292.3012; found, 292.1072; anal. calcd for $C_{15}H_{12}N_6O$: C, 61.64; H, 4.14; N, 28.75; O, 5.47; found: C, 61.65; H, 4.13; N, 28.76; O, 5.46%.

2-Methyl-N-(pyridazin-4-yl)-6-(pyrimidin-5-ylamino)benzamide (3z). 92.6% yield; mp 223–235 °C; 1H NMR (300 MHz, $CDCl_3$) δ : 10.37 (s, 1H, –NH–N), 9.61 (s, 1H, –CH–N), 9.30 (m, 1H, –CH–N), 9.23 (s, 1H, –NH–), 8.90 (s, 1H, –N–CH–), 8.50 (s, 2H, –CH==N), 8.29 (m, 1H, Ph–H), 7.40 (m, 1H, Ph–H), 6.90 (m, 1H, Ph–H), 2.48 (s, 3H, –CH₃); ^{13}C NMR (75 MHz, $CDCl_3$) δ : 164.7, 150.4, 147.4, 144.2, 143.8, 143.7, 143.1, 142.9, 139.4, 138.0, 121.5, 120.8, 114.2, 113.4, 18.1; HR-ESI-MS m/z : calcd for $C_{16}H_{14}N_6O$ ($[M + H]^+$), 306.3302; found, 306.1229; anal. calcd for $C_{16}H_{14}N_6O$: C, 62.74; H, 4.61; N, 27.43; O, 5.22; found: C, 62.75; H, 4.60; N, 27.42; O, 5.23%.

4.2. Biological activity

4.2.1. Biological activity screening *in vitro*. The tumor cells (human lung cancer cells H1975 and A549, and cervical cancer cells Hela; from Chongqing Institute of Chinese Materia Medica) were extended, logarithmic phase cells were collected, the concentration of the cell suspensions was adjusted, and 100 μ L was added to each hole so that the test cells were plated to a density modulation of 5000 cell per hole ceiling. The plates were transferred to a CO₂ incubator and incubated at 37 °C under 5% CO₂ and saturated humidity conditions until a cell monolayer covered the hole bottom, using a drug concentration gradient dilution of 5, adding MTT solution (20 μ L, 5 mg mL⁻¹; 0.5% MTT) to each hole, and culturing for 3–4 h. After termination of cell culture coloration, the hole broth was carefully aspirated, DMSO (150 μ L) was added, and the mixture was subjected to low speed vibration for 10 min on shaking bed to fully dissolve the crystals. The standard deviation of all raw data (OD value) (SD) was analyzed, the mean of each group was used to replace the large deviation data and calculate the inhibition rate, and the IC₅₀ value was derived using specialized software based on the drug concentration and corresponding inhibition. Sorafenib and



sunitinib were used as positive controls in the *in vitro* experiment. Data were analyzed by linear regression using statistical software SPSS (version 13.0).

4.2.2. Biological activity evaluation *in vivo*. Logarithmic growth stages of tumor cells (human lung cancer A549 and human cervical cancer Hela) were used to prepare cell suspensions and inoculated under the right axilla of 50 nude mice. Nude mice were randomly assigned to drug feeding after tumor growth of 100–200 mm³. Drug administration included activity screening of compounds *in vitro* (doses: 10, 50, and 100 mg kg⁻¹ d⁻¹) using positive controls (sorafenib and sunitinib; 50 mg kg⁻¹ d⁻¹) and a blank controls (DMSO, 50 mg kg⁻¹ d⁻¹). Medication was administered orally once a day for 15 consecutive days. The antitumor effect on nude mice was observed dynamically by measuring tumor diameter. The number of tumor diameter measurements (2–3 times a week) was based on growth of the transplanted tumor. The relative tumor proliferation rate (T/C, %) was used as the evaluation index for antitumor activity *in vivo*. Data were analyzed by linear regression using statistical software SPSS (version 13.0).

Live subject statement

All animal procedures were performed in accordance with the Guidelines for Care and Use of Laboratory Animals of "Chongqing Institute of Chinese Materia Medica" and experiments were approved by the Animal Ethics Committee of "Chongqing Institute of Chinese Materia Medica".

Conflicts of interest

There are no conflicts to declare.

Acknowledgements

This work was sponsored by the Innovation Team Project of Universities in Chongqing (No. CXTDX201601018), the Chongqing Scientific and Technological Innovation Special Project of Social Undertakings and People's Livelihood Guarantee (No. cstc2015shmszx80060), the Chongqing University Students' Training Project of Innovation and Undertaking (201510637085), the Doctoral Program of Chongqing Normal University (No. 12XLB006), and the Outstanding Achievements Transformation Project of Chongqing Normal University (No. 15XZH08), and the National Natural Science Foundation (21662012, 41866005), China.

References

- 1 A. Birbrair, T. Zhang, Z. Wang, *et al.*, Type-2 pericytes participate in normal and tumoral angiogenesis, *Am. J. Physiol.: Cell Physiol.*, 2014, **307**, C25–C38.
- 2 E. Lee, J. Locker, M. Nalesnik, *et al.*, The association of Epstein-Barr virus with smooth-muscle tumors occurring after organ transplantation, *N. Engl. J. Med.*, 1995, **332**, 19–25.
- 3 D. Ambrosi and F. Mollica, On the mechanics of a growing tumor, *Int. J. Eng. Sci.*, 2002, **40**, 1297–1316.
- 4 K. Volokh, Stresses in growing soft tissues, *Acta Biomater.*, 2006, **2**, 493–504.
- 5 C. Bernstein, A. Prasad, V. Nfonsam, *et al.*, DNA Damage, DNA Repair and Cancer, *New Res Dir DNA Repair*, 2013, Vol. 5, pp. 413–465.
- 6 M. Kastan, DNA damage responses: mechanisms and roles in human disease: 2007 G.H.A. Clowes Memorial Award Lecture, *Mol. Cancer Res.*, 2008, **6**, 517–524.
- 7 F. Cunningham, S. Fiebelkorn, M. Johnson, *et al.*, A novel application of the Margin of Exposure approach: segregation of tobacco smoke toxicants, *Food Chem. Toxicol.*, 2011, **49**, 2921–2933.
- 8 H. Kanavy and M. Gerstenblith, Ultraviolet radiation and melanoma, *Semin. Cutaneous Med. Surg.*, 2011, **30**, 222–228.
- 9 O. Handa, Y. Naito and T. Yoshikawa, Redox biology and gastric carcinogenesis: the role of Helicobacter pylori, *Redox Rep.*, 2011, **16**, 1–7.
- 10 C. Bernstein, H. Holubec, A. Bhattacharya, *et al.*, Carcinogenicity of deoxycholate, a secondary bile acid, *Arch. Toxicol.*, 2011, **85**, 863–871.
- 11 M. Katsurano, T. Niwa, Y. Yasui, *et al.*, Early-stage formation of an epigenetic field defect in a mouse colitis model, and non-essential roles of T-cells and B-cells in DNA methylation induction, *Oncogene*, 2012, **31**, 342–351.
- 12 D. Malkin, Li-fraumeni syndrome, *Genes Cancer*, 2011, **2**, 475–484.
- 13 P. Lichtenstein, N. Holm, P. Verkasalo, *et al.*, Environmental and heritable factors in the causation of cancer-analyses of cohorts of twins from Sweden, Denmark, and Finland, *N. Engl. J. Med.*, 2000, **343**, 78–85.
- 14 L. Shen, Y. Kondo, G. Rosner, *et al.*, MGMT promoter methylation and field defect in sporadic colorectal cancer, *J. Natl. Cancer Inst.*, 2005, **97**, 1330–1338.
- 15 K. Truninger, M. Menigatti, J. Luz, *et al.*, Immunohistochemical analysis reveals high frequency of PMS2 defects in colorectal cancer, *Gastroenterology*, 2005, **128**, 1160–1171.
- 16 N. Valeri, P. Gasparini, M. Fabbri, *et al.*, Modulation of mismatch repair and genomic stability by miR-155, *Proc. Natl. Acad. Sci. U. S. A.*, 2005, **102**, 6982–6987.
- 17 A. Facista, H. Nguyen, C. Lewis, *et al.*, Deficient expression of DNA repair enzymes in early progression to sporadic colon cancer, *Genome Integr.*, 2012, **3**, 3.
- 18 C. Bernstein, H. Bernstein, C. Payne, *et al.*, Field defects in progression to gastrointestinal tract cancers, *Cancer Lett.*, 2008, **260**, 1–10.
- 19 H. Rubin, Fields and field cancerization: the preneoplastic origins of cancer: asymptomatic hyperplastic fields are precursors of neoplasia, and their progression to tumors can be tracked by saturation density in culture, *BioEssays*, 2011, **33**, 224–231.
- 20 B. Vogelstein, N. Papadopoulos, V. Velculescu, *et al.*, Cancer genome landscapes, *Science*, 2013, **339**, 1546–1558.
- 21 P. Lochhead, A. Chan, R. Nishihara, *et al.*, Etiologic field effect: reappraisal of the field effect concept in cancer predisposition and progression, *Mod. Pathol.*, 2014, **28**, 14–29.



22 G. Manning and D. Whyte, The protein kinase complement of the human genome, *Science*, 2002, **298**, 1912–1934.

23 V. Reiterer, P. Eyers and H. Farhan, Day of the dead: pseudokinases and pseudophosphatases in physiology and disease, *Trends Cell Biol.*, 2014, **24**, 489–505.

24 J. Murphy, A robust methodology to subclassify pseudokinases based on their nucleotide-binding properties, *Biochem. J.*, 2014, **457**, 323–334.

25 P. Eyers and J. Murphy, The evolving world of pseudoenzymes: proteins, prejudice and zombies, *BMC Biol.*, 2016, **14**, 98.

26 N. Dhanasekaran and R. Premkumar, Signaling by dual specificity kinases, *Oncogene*, 1998, **17**, 1447–1455.

27 P. Besant, E. Tan and P. Attwood, Mammalian protein histidine kinases, *Int. J. Biochem. Cell Biol.*, 2003, **35**, 297–309.

28 T. Stout, P. Foster and D. Matthews, High-throughput structural biology in drug discovery: protein kinases, *Curr. Pharm. Des.*, 2004, **10**, 1069–1082.

29 O. Linden, A. Kooistra, R. Leurs, *et al.*, KLIFS: A knowledge-based structural database to navigate kinase-ligand interaction space, *J. Med. Chem.*, 2013, **57**, 249–277.

30 S. Hanks, Genomic analysis of the eukaryotic protein kinase superfamily: a perspective, *Genome Biol.*, 2003, **4**, 111.

31 D. Knighton, J. Zheng, E. Ten, *et al.*, Crystal structure of the catalytic subunit of cyclic adenosine monophosphate-dependent protein kinase, *Science*, 1991, **253**, 407–414.

32 S. Vlahopoulos and V. Zoumpourlis, JNK: a key modulator of intracellular signaling, *Biochemistry*, 2004, **69**, 844–854.

33 Q. Xu, K. Malecka, L. Fink, *et al.*, Identifying three-dimensional structures of autophosphorylation complexes in crystals of protein kinases, *Sci. Signaling*, 2015, **8**, rs13.

34 P. Wolanin, P. Thomason and J. Stock, Histidine protein kinases: key signal transducers outside the animal kingdom, *Genome Biol.*, 2002, **3**, 1–8.

35 F. Yakes, J. Chen, J. Tan, *et al.*, Cabozantinib (XL184), a novel MET and VEGFR2 inhibitor, simultaneously suppresses metastasis, angiogenesis, and tumor growth, *Mol. Cancer Ther.*, 2011, **10**, 2298–2308.

36 G. Roth, A. Heckel, F. Colbatzky, *et al.*, Design, synthesis, and evaluation of indolinones as triple angiokinase inhibitors and the discovery of a highly specific 6-methoxycarbonyl-substituted indolinone(BIBF 1120), *J. Med. Chem.*, 2009, **52**, 4466–4480.

37 Y. Oguro, N. Miyamoto, K. Okada, *et al.*, Design, synthesis, and evaluation of 5-methyl-4-phenoxy-5H-pyrrolo [3, 2-d] pyrimidine derivatives: novel VEGFR2 kinase inhibitors binding to inactive kinase conformation, *Bioorg. Med. Chem.*, 2010, **18**, 7260–7273.

38 K. Sanphanya, S. Wattanapitayakul, S. Phowichit, *et al.*, Novel VEGFR2 kinase inhibitors identified by the back-to-front approach, *Bioorg. Med. Chem. Lett.*, 2013, **23**, 2962–2967.

39 W. Lin, J. Hsu, S. Hsieh, *et al.*, Discovery of 3-phenyl-1H-5-pyrazolylamine derivatives containing a urea pharmacophore as potent and efficacious inhibitors of FMS-like tyrosine kinase-3 (FLT3), *Bioorg. Med. Chem.*, 2013, **21**, 2856–2867.

40 T. Cho, S. Dong, F. Jun, *et al.*, Novel potent orally active multitargeted receptor tyrosine kinase inhibitors: synthesis, structure-activity relationships, and anti-tumor activities of 2-indolinone derivatives, *J. Med. Chem.*, 2010, **53**, 8140–8149.

41 R. Hudkins, A. Zulli, T. Underiner, *et al.*, 8-THP-DHI analogs as potent type I dual TIE-2/VEGFR2 receptor tyrosine kinase inhibitors, *Bioorg. Med. Chem. Lett.*, 2010, **20**, 3356–3360.

42 B. Yu, L. Tang, Y. Li, *et al.*, Design, synthesis and anti-tumor activity of 4-aminoquinazoline derivatives targeting VEGFR2 tyrosine kinase, *Bioorg. Med. Chem. Lett.*, 2012, **22**, 110–114.

43 P. Plé, F. Jung, S. Ashton, *et al.*, Discovery of AZD2932, a new quinazoline ether inhibitor with high affinity for VEGFR2 and PDGFR tyrosine kinases, *Bioorg. Med. Chem. Lett.*, 2012, **22**, 262–266.

44 S. Rizvi, H. Siddiqui, M. Nisar, *et al.*, Discovery and molecular docking of quinolyl-thienyl chalcones as antiangiogenic agents targeting VEGFR2 tyrosine kinase, *Bioorg. Med. Chem. Lett.*, 2012, **22**, 942–944.

45 A. Kiselyov, M. Semenova and V. Semenov, 3, 4-Disubstituted isothiazoles: novel potent inhibitors of VEGF receptors 1 and 2, *Bioorg. Med. Chem. Lett.*, 2009, **19**, 1195–1198.

46 Y. Oguro, D. Cary, N. Miyamoto, *et al.*, Design, synthesis, and evaluation of novel VEGFR2 kinase inhibitors: discovery of [1, 2, 4] triazolo [1, 5-a] pyridine derivatives with slow dissociation with slow dissociation kinetics, *Bioorg. Med. Chem.*, 2013, **21**, 4714–4729.

47 A. Gangjee, N. Zaware, S. Raghavan, *et al.*, Synthesis and biological activity of 5-chloro-N-4- substituted phenyl-9H-pyrimido [4, 5-b] indole-2, 4-diamines as vascular endothelial growth factor receptor-2 inhibitors and antiangiogenic agents, *Bioorg. Med. Chem.*, 2013, **21**, 1857–1864.

48 Q. Liu, Y. Sabnis, Z. Zhao, *et al.*, Developing irreversible inhibitors of the protein kinase cisteinome, *Chem. Biol.*, 2013, **20**, 146–159.

49 A. Wissner, H. Fraser, C. Ingalls, *et al.*, Dual irreversible kinase inhibitors: quinazoline-based inhibitors incorporating two independent reactive centers with each targeting different cysteine residues in the kinase domains of EGFR and VEGFR2, *Bioorg. Med. Chem.*, 2007, **15**, 3635–3648.

50 S. Kumar and M. Tiwari, Topomer-CoMFA-based predictive modelling on 2,3-diaryl substituted-1,3-thiazolidin-4-ones as non-nucleoside reverse transcriptase inhibitors, *Med. Chem. Res.*, 2015, **24**, 245–257.

